Measurement of Thermal Conductivity and Viscosity of a ZrO_2-TiO_2 Hybrid Nanofluid for Heat Transfer Applications

J. Anandakumar*, K. Palaniradja and N. Alagumurthi
Department of Mechanical Engineering, Puducherry Technological University, Puducherry, India.
*Corresponding author (e-mail: anandakumar.j@pec.edu)

Heat transfer techniques utilizing nanofluids have been developed. Various metallic and ceramic nanofluids with water have been thoroughly investigated for their thermal applications. The current study deals with the synthesis of zirconium dioxide (ZrO_2) and titanium dioxide (TiO_2) hybrid nanofluids through a two-step process. Nanoparticle volume fractions (50% of ZrO_2 and 50% of TiO_2 by volume) and concentrations of 0.5, 1 and 1.5 % by weight were created for this purpose. The thermal conductivity (TC) and viscosity (VC) of hybrid nanofluids made using various volume fractions were measured at temperatures ranging from 25 to 60 °C. X-ray diffraction (XRD) showed that the materials produced were monoclinic ZrO_2 and TiO_2. Nanoparticles were characterized by XRD, SEM (Scanning Electron Microscopy) and EDX (Energy Dispersive X-Ray) with mapping and FTIR (Fourier Transform Infrared Spectroscopy). SEM scans revealed that the nanoparticles were irregularly shaped and strongly agglomerated.

Keywords: Zirconium dioxide; titanium dioxide; hybrid nanofluid; viscosity; heat transfer; thermal conductivity

Received: November 2022; Accepted: February 2023

Many industries depend on heating and cooling fluids, including the power, transportation, and electronics industries. All high-energy equipment must have appropriate cooling systems to work. Owing to their low heat transfer properties, common fluids for heat transfer such as oil, water, and ethylene glycol (EG) have a limited capacity for carrying heat. However, solid particles have superior thermal conductivity (TC) to most fluids, and their dispersion in a liquid improves its heat transmission qualities. Colloidal suspensions comprising metal, nitride, carbon nanotube, or metal oxide particles smaller than 100 nm in size, diluted in a base fluid such as EG, refrigerants, and water, are known as nanofluids. Many researchers are investigating more effective techniques for improving the thermal performance of heat transfer fluids [1–3]. A helical coil heat exchanger utilizing CuO, TiO_2, and Al_2O_3/water nanofluids has also been investigated. The efficiency of heat exchangers may be improved by adding nano-particles into water [4]. A study found that the pressure drop was 9 % larger than that of water at a concentration of 0.8 % [5]. According to a report, base fluids and nano- fluids have higher convectional heat transfer coefficients. Nanofluids of EG with 1 % copper nanoparticles need less coolant pumping power than the base fluid [6]. Synthesizing an Al_2O_3-Cu nanocomposite utilizes a thermochemical process. By dispersing it in deionized water, hybrid nanofluids may be created to the necessary volume. Thus, the viscosity (VC) and TC values for the hybrid fluids are much more significant than those predicted by theoretical models [7]. Based on comparative calculations from statistical processes and mixing theory, the results were favourable. The grain size, surface area, porosity, and porosity interface layer may be responsible [8]. On the viability of employing an air-cooled heat exchanger, an Al_2O_3 nanofluid from a renewable energy source is being researched. The maximum heat exchange was 0.325 kW, equivalent to 60 ºC in temperature and 2.4 L/min pumping power. The enhanced heat capacity ratio dropped as the intake temperature rose, but the pumping power ratio increased [9].

Nanofluids consisting of graphene and water may improve heat transmission using less power [10]. The TC values of Al_2O_3/H_2O nanofluids at various particle concentrations were reported using the KD2 Pro thermal property analysis tool. Viscosity significantly increased as nanoparticle concentration increased. TC values increased by 9.44 and 13.22 % when compared to volume concentrations [11]. Numerous studies have examined the TC of nano-fluids with metal or metal oxide particles [12–15]. 0.1, 0.2 and 0.3 % volume fractions of ZrO_2/H_2O nano-fluids were tested using a KD2 Pro device to determine their TC. The obtained VC values were proportional to the nanoparticle concentrations [16]. Nanofluids were measured at different concentrations in the base fluid because they often have better thermophysical properties than other materials. The characteristics imply that the studied samples were more appropriate for thermal management applications [17, 18]. A two-step technique was utilized to create nanofluids in EG. The TC of ZrO_2/EG was calculated using a thermal property analyzer with five different volume concentrations. Heat transport was predicted to be significantly influenced by ZrO_2 nanoparticles [19]. Concentrations between 0.5 and 1.5 vol%. 20 to 60°C were used to study the TC and VC of hybrid nanofluids [20].

The TC and dynamic viscosity of SiO_2-TiO_2 nanofluids have been experimentally investigated. The sample with the greatest stability required 90 minutes of sonication time and had an absorbance ratio of over 70 % [21]. A thermal property analyzer like the KD2 Pro can determine the TC values associated with nanofluids at various temperature ranges. When the experimental data and several models were evaluated, it was discovered that the estimated values from the theoretical models were much lower than the observed values [22–26]. Several researchers reviewed the characteristics of nanofluids and potential issues. Convective heat transfer may be increased by various methods, including changing the flow's form and boundary conditions or improving the actual fluid's TC. From the literature, titanium dioxide and zirconium dioxide nanofluids have solid thermal conductance and efficient heat transfer capabilities, making them ideal for thermal engineering applications [27–30].

In this work, ZrO_2-TiO_2 hybrid nanofluids were synthesised utilizing a two-step process. Characterization was performed using SEM, EDX with mapping, XRD, and FTIR analysis.

EXPERIMENTAL

Synthesis and Preparation of ZrO_2-TiO_2 Hybrid Nanofluid

In this work, a combination of ZrO_2 and TiO_2 hybrid nanofluids was used to generate various nanoparticle concentrations utilizing a two-step process of nanoparticle dispersion in the underlying fluid [7]. Nanofluids were made with two distinct nanoparticle volume fractions (50% of ZrO_2 and 50% of TiO_2 by volume) and concentrations of 0.5, 1 and 1.5 % by weight were created for this purpose. Pre-weighed quantities of nanoparticles were dispersed in 1000 ml of distilled water as the base fluid to create the sample nanofluids. This approach is used to synthesize nanofluids by combining essential fluids. This technology is inexpensive and suited for large-scale manufacturing since it uses processes often utilized in industries. **Table 1** shows the details of the ZrO_2 and TiO_2 nanoparticles. A graphic representation of the hybrid nanofluid preparation process is provided in **Figure 1**. Equation 1 was explicitly computed and reassessed to measure the exact equilibrium of the nanoparticles employed [19].

$$\% \text{ Volume concentration} = \frac{\frac{W_{nanoparticle}}{\rho_{nanoparticle}}}{\frac{W_{nanoparticle}}{\rho_{nanoparticle}} + \frac{W_{basefluid}}{\rho_{basefluid}}} \quad \text{(Equation 1)}$$

where ρ = density and W = weight

Table 1. Details of nanoparticles.

Sl. No	Nanoparticle	Size	Manufacturer
1	ZrO_2	100 nm	Sigma-Aldrich
2	TiO_2	100 nm	Sigma-Aldrich

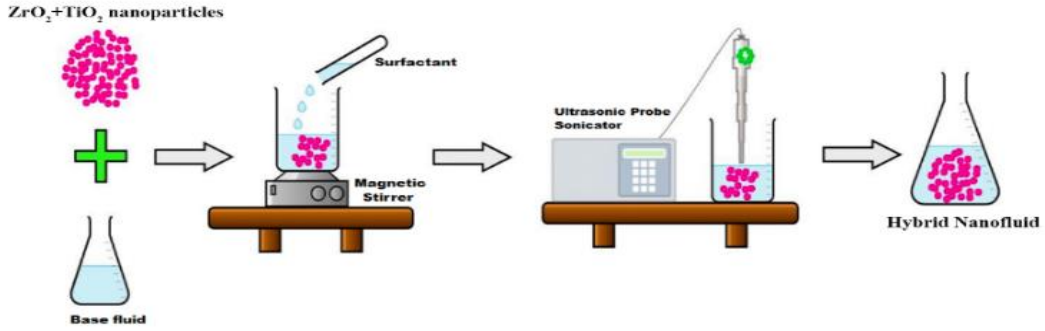

Figure 1. Preparation process of hybrid nanofluids.

Figure 2. Sonication of hybrid nanofluids.

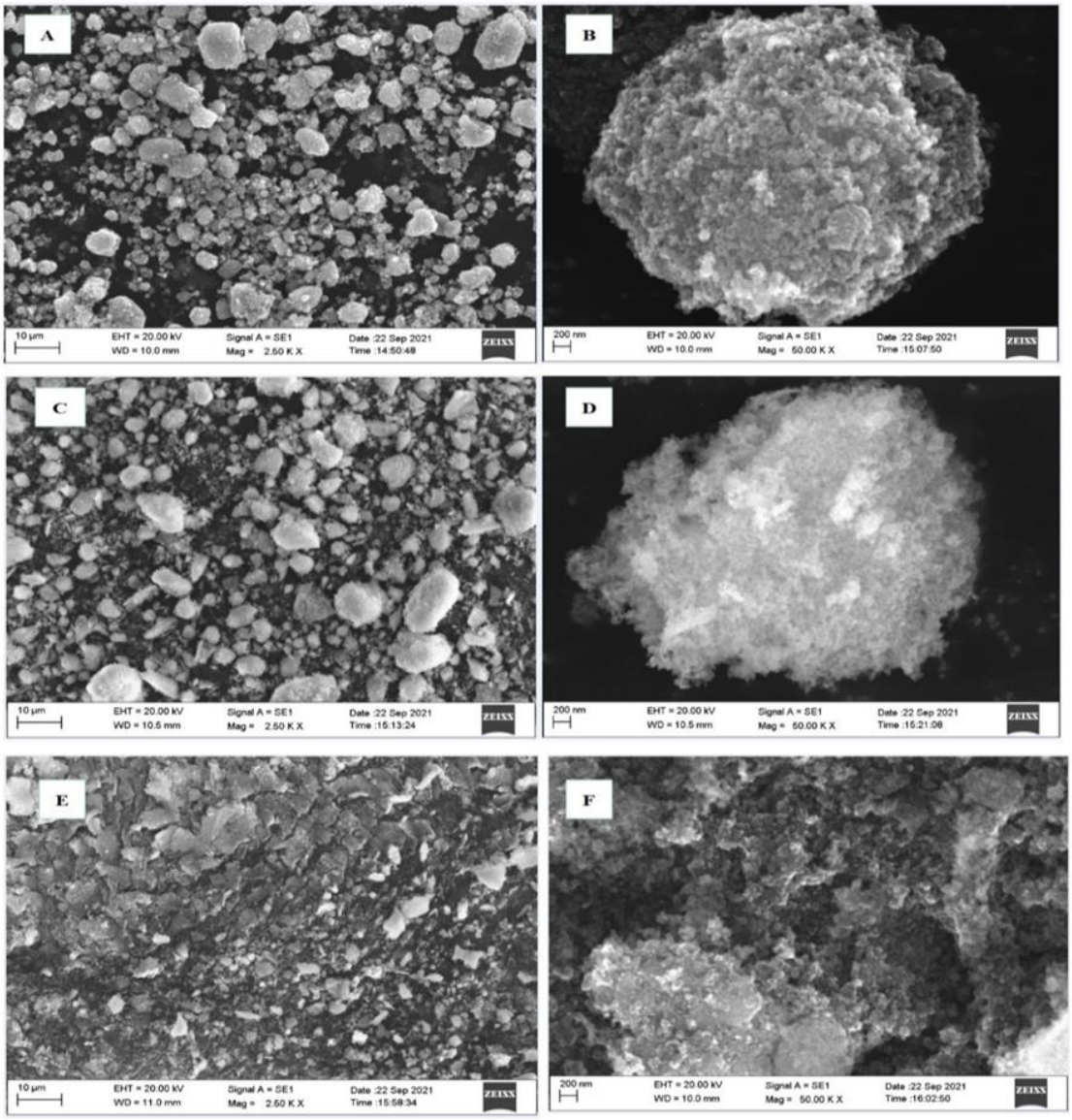

Figure 3. (A, B) SEM images of TiO_2 nanoparticles at two magnifications (250 K X and 50 K X). (C, D) SEM images of ZrO_2 nanoparticles at two magnifications (250 K X and 50 K X). (E, F) SEM images of (ZrO_2-TiO_2) nanoparticles at two magnifications (250 K X and 50 K X).

The two different nanoparticle concentrations necessary were created by combining distilled water with a mixed solution of nanoparticles using an ultrasonic probe sonicator at 180 W and 40 kHz for 180 minutes. This process breaks down large agglomerates [1]. A surfactant was added to boost the nanofluid's stability. **Figure 2** illustrates that hybrid nanofluids were sonicated using an ultrasonicator.

Material Characterization

SEM Analysis

The SEM images of the synthesized ZrO_2 and TiO_2 nanoparticles are shown in **Figure 3**. To analyze the real surface morphology of the ZrO_2 and TiO_2 nanoparticles, we used an SEM (ZEISS EVO18) at 0.2 to 30 kV of accelerating voltage and an analytical working distance (AWD) of 6 mm. The size and dispersion of the particles and microstructural analysis provided quality control and a critical analytical tool for assessing grain structures. The SEM photos demonstrate that the nanoparticle aggregation increased the size of the ZrO_2 and TiO_2 nanoparticles and that their shapes were uniformly spherical.

EDX with Mapping Analysis

EDX (Energy Dispersive X-Ray) line mapping was crucial for confirming the composition of the nanoparticles. The elemental line mapping for the combination of ZrO_2-TiO_2 nanoparticles is seen in **Figure 4**. Three colours (red, yellow and green) appear in these mapping images. Red represents the zirconium (Zr) component, yellow represents the titanium (Ti) component, and green represents the oxide (O) component. The EDX spectrum supported these findings.

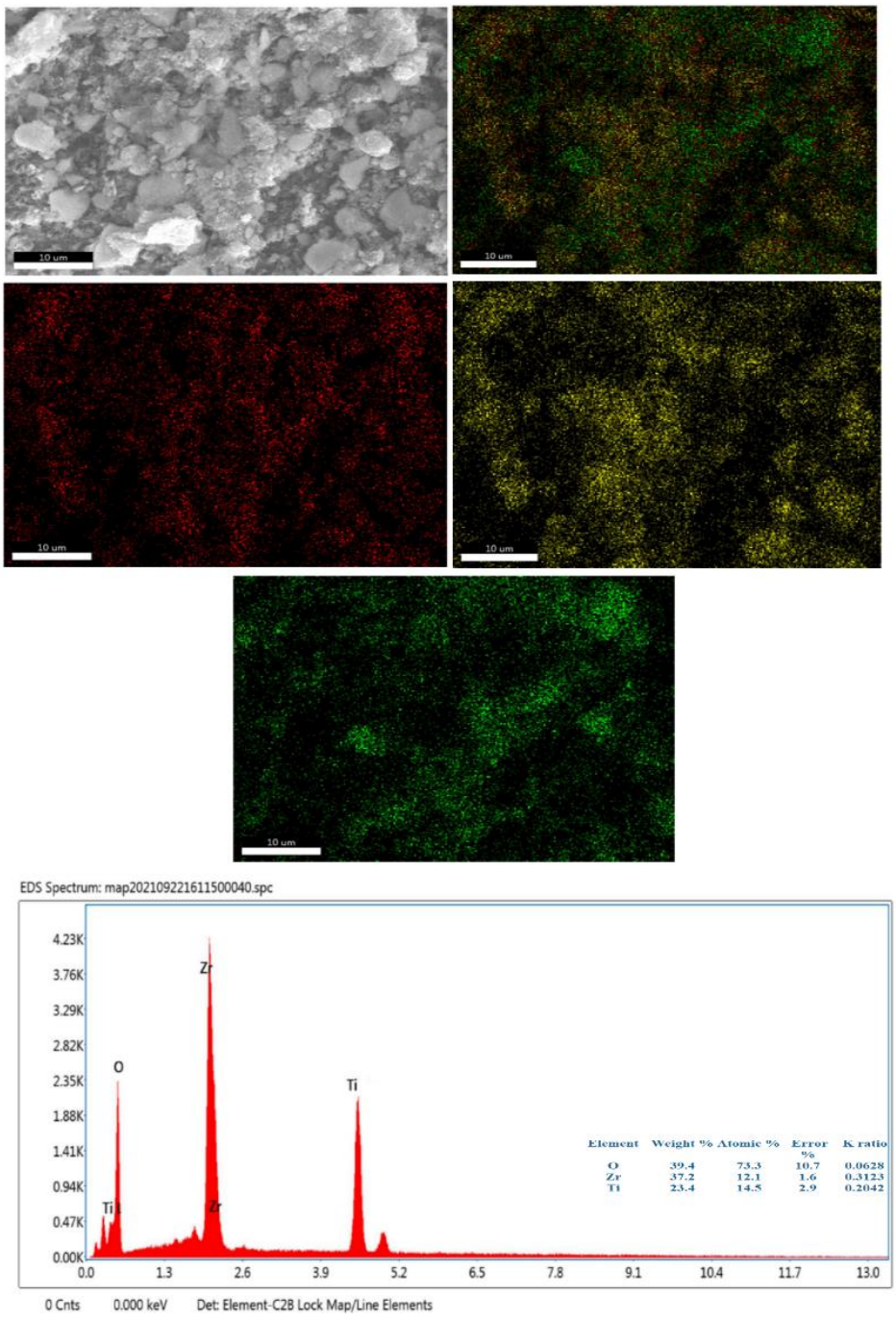

Figure 4. EDX analysis of (ZrO_2-TiO_2) nanoparticles.

XRD Analysis

The ZrO_2 and TiO_2 nanoparticle powders were subjected to X-ray Diffraction (XRD) analysis (D8 Advance ECO). CuKα radiation (1.54 A) was employed at a voltage of 40 kV and 25 mA of current. The ZrO_2 and TiO_2 nanoparticles' XRD patterns are shown in **Figure 5** and **Figure 6**. The apparent peaks of the nanoparticles showed excellent crystallinity; no distinctive peaks of any other phase of the nanoparticles were seen and these were consistent with JCPDS card no. 32-1498 for ZrO_2 and JCPDS card no. 88-1175 for TiO_2. X-ray diffraction analysis confirmed the synthesized materials to be ZrO_2 and TiO_2 nanoparticles. All diffraction peaks coincided with those of monoclinic ZrO_2 and TiO_2 nanoparticles. The findings were consistent with previously published studies [18, 31]. The Debye-Scherrer formula shown in Equation 2 was used to determine the typical crystal sizes of the nanoparticles, which were 29 nm for ZrO_2 and 27 nm for TiO_2.

$$D = \frac{0.89\lambda}{\beta \cos\theta} \qquad \text{(Equation 2)}$$

where β is the peak width, D is the size of the crystallite, θ is the Bragg angle associated with the peak, and λ is the wavelength of the X-ray radiation.

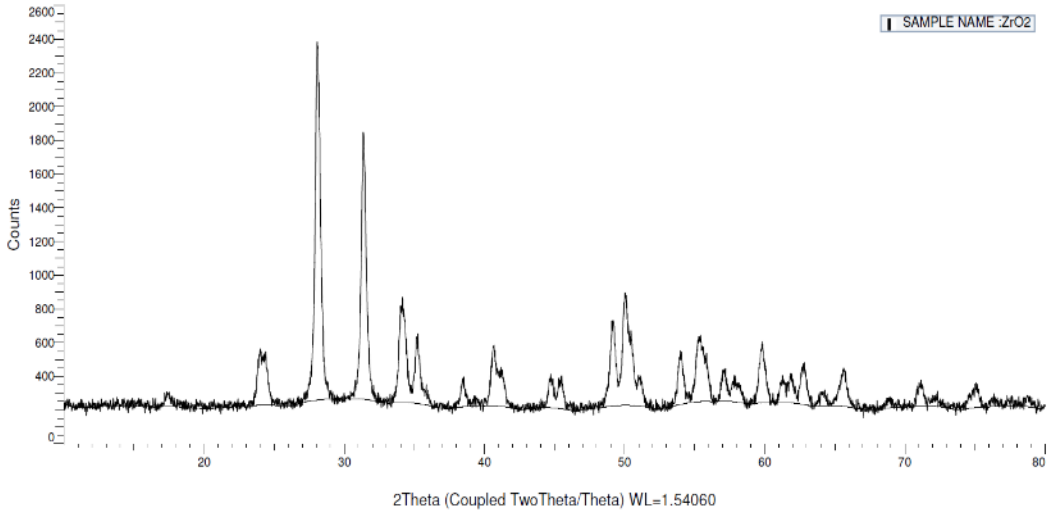

Figure 5. XRD pattern of ZrO_2 nanoparticles.

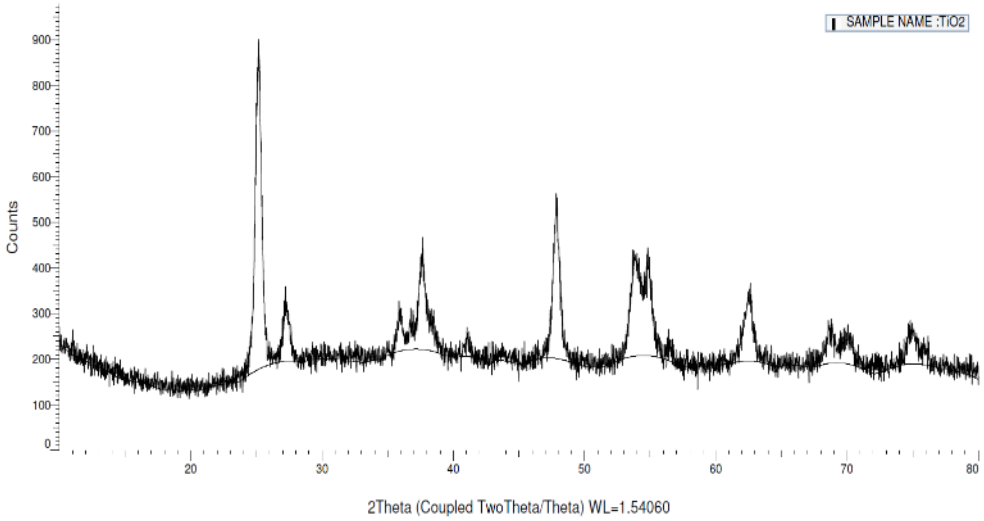

Figure 6. XRD pattern of TiO_2 nanoparticles.

FTIR Analysis

FTIR (Fourier Transform infrared spectroscopy) was utilized to assess the samples [32]. The FTIR spectra of the ZrO_2 and TiO_2 nanoparticles are shown in **Figure 7** and **Figure 8**. As a result of OH stretching, the spectra of ZrO_2 and TiO_2 nanoparticles displayed strong peaks at 3421.72 cm^{-1} and 3415.26 cm^{-1}. The occurrence of separate peaks at 1629.85 cm^{-1} and 1625.99 cm^{-1} suggested the presence of H_2O molecules or the OH bend. ZrO_2 showed a broad peak at 443.63 cm^{-1} and 574.79 cm^{-1}, equivalent to the Zr-O band and Zr-O-Zr. The Ti-O band and Ti-O-Ti were represented by the broad peaks of TiO_2 at 414.70 cm^{-1} and 746.45 cm^{-1}.

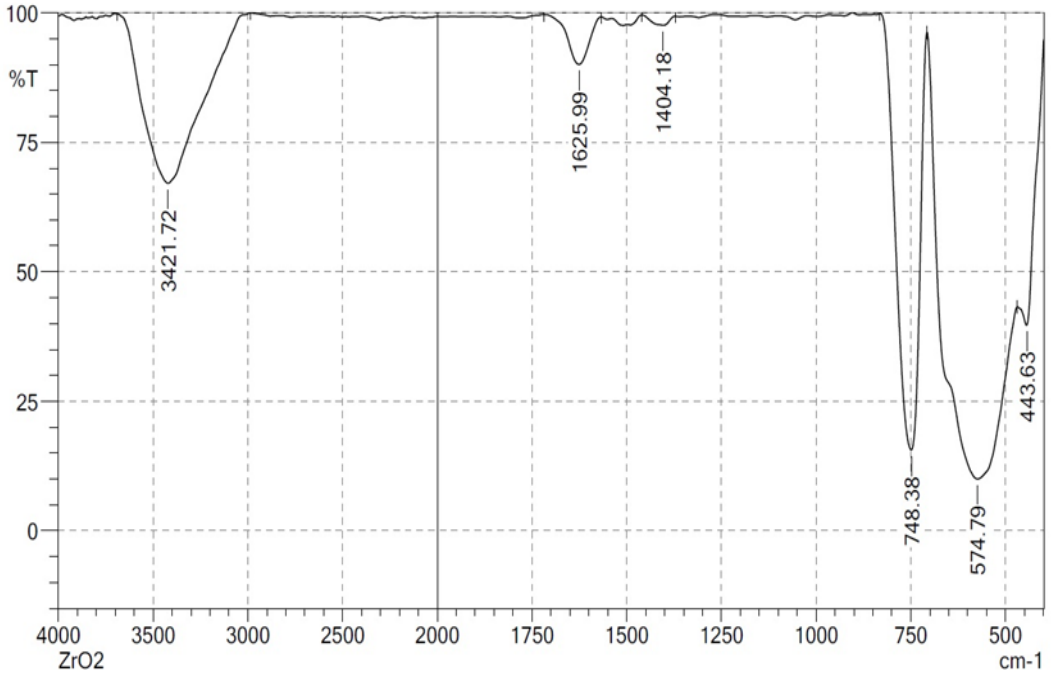

Figure 7. FTIR spectrum of ZrO_2 nanoparticles.

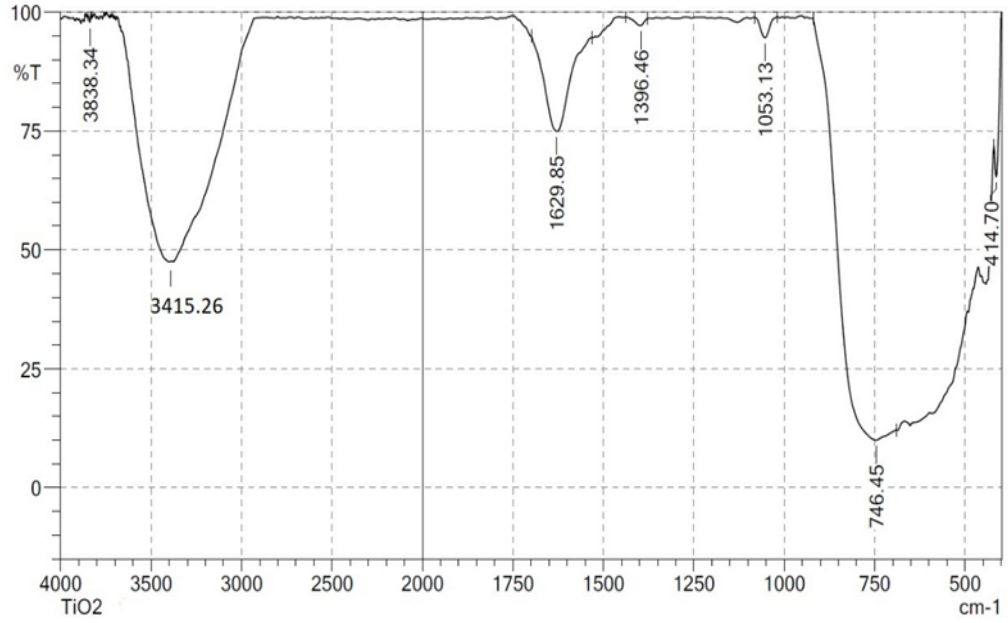

Figure 8. FTIR spectrum of TiO_2 nanoparticles.

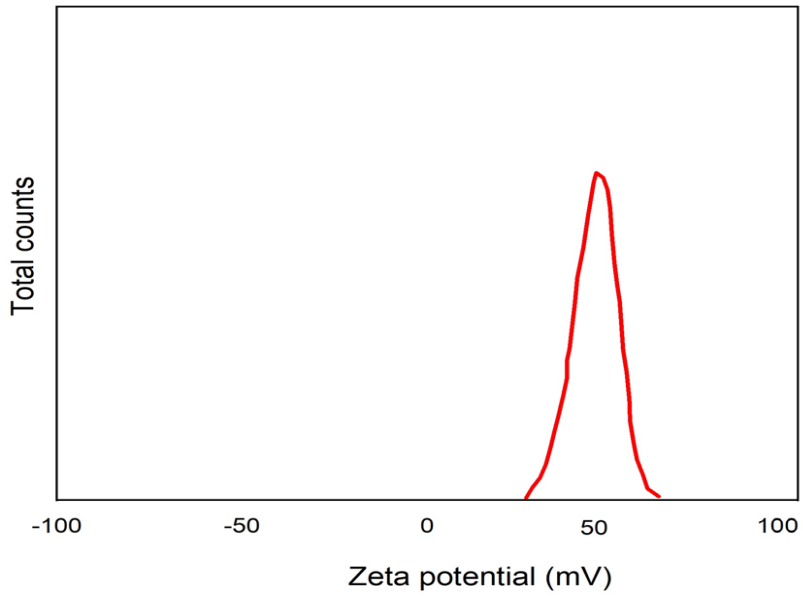

Figure 9. Zeta potential distribution

Zeta Potential

The suspension stability of the hybrid nanofluid sample was examined based on room-temperature zeta potential findings. Zeta potential values above 50 mV imply good suspension stability [19]. The Zeta Potential distribution plot is shown in **Figure 9.**

Measurement of Hybrid Nanofluids

Thermal Conductivity (TC) Measurement

In order to evaluate the TC of the ZrO_2-TiO_2 hybrid nanofluids, the KD2 Pro, a battery-powered, menu-driven device with sensor needles and a portable microprocessor, was employed (Decagon Devices, Inc., USA). The KD2 sensor needle contains a heating element and thermistor. The sensor needle can measure the TC of fluids with ±5 % accuracy within the range of 0.2-2 W/mK. A thermal needle probe instrument was used for initial calibration in the experimental procedure to ascertain the actual TC of the nanofluid. This calibration process was carried out using glycerine and water. To ensure temperature accuracy, a 45 ml nanofluid sample was sealed in a 30 mm diameter vial, and the test tube was connected. During this procedure, a probe was put vertically into the sealed vial's predrilled hole. When the sample reaches an equilibrium temperature in 5 to 10 minutes, it is crucial to check that the thermal probe is well immersed in the sample. At each specific fluid temperature, a minimum of five observations with 15-minute intervals were recorded. Glass wool insulation 25 mm thick was used to prevent heat escaping freely into the surroundings and to slow down heat loss throughout this operation. A broad range of temperatures (25–60 ºC) was used for the TC measurements. The experimental setup is shown in **Figure 10**.

Figure 10. TC measurement of hybrid nanofluids.

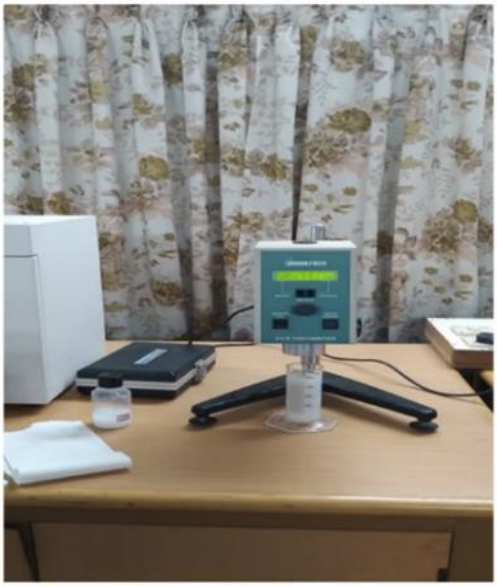

Figure 11. VC measurement of hybrid nanofluids.

Viscosity (VC) Measurement

A Brookfield DV-E Viscometer was used to test the VC of several heat transfer fluids in this study. The Brookfield DV-E is a rotational digital viscometer with an LCD (**Figure 11**). This viscometer can continuously sense and display without user intervention. The torque needed to spin an immersed element in a fluid is measured using the viscometer. A motor drives the spindle through a calibrated spring. The computerized display shows the spring's deflection. The viscous drag, or flow resistance, is proportional to the spindle speed and is affected by spindle size and form. The drag rises as the rotating speed increases. The spindle speed is modified for a specific test fluid to evaluate the change in VC with rotational speed. Different spindles may be utilized to achieve different VC ranges.

RESULTS AND DISCUSSION

Thermal Conductivity (TC) Analysis of Hybrid Nanofluids

TC is the most important parameter in the practical application of hybrid nanofluids. There are presently no theoretical formulations that can compute the TC of hybrid nanofluids with any certainty, even though numerous studies have reported theoretical and practical values for the TC of nanofluids. Many investigations have been undertaken to analyse the effective solid-state TC distributed in base solutions. In this study, TC was determined in hybrid nanofluids (ZrO_2-TiO_2) of 0.5, 1.0, and 1.5 % concentrations. The calculation of TC employs the Bruggeman model shown in Equation 3. It suggests that TC and nanoparticle concentration are inversely related [33].

$$k_{effective} = \frac{k_{basefluid}}{4}\left[(3\phi - 1)\frac{k_{nanoparticle}}{k_{basefluid}} + (2 - 3\phi) + \frac{k_{basefluid}}{4}\sqrt{\Delta}\right] \quad \text{(Equation 3)}$$

Where

$$\Delta = \left[(3\phi - 1)^2\left(\frac{k_{nanoparticle}}{k_{basefluid}}\right) + (2 - 3\phi)^2 + 2(2 + 9\phi^2)\left(\frac{k_{nanoparticle}}{k_{basefluid}}\right)\right]$$

ϕ = Volume fraction and K = Thermal conductivity

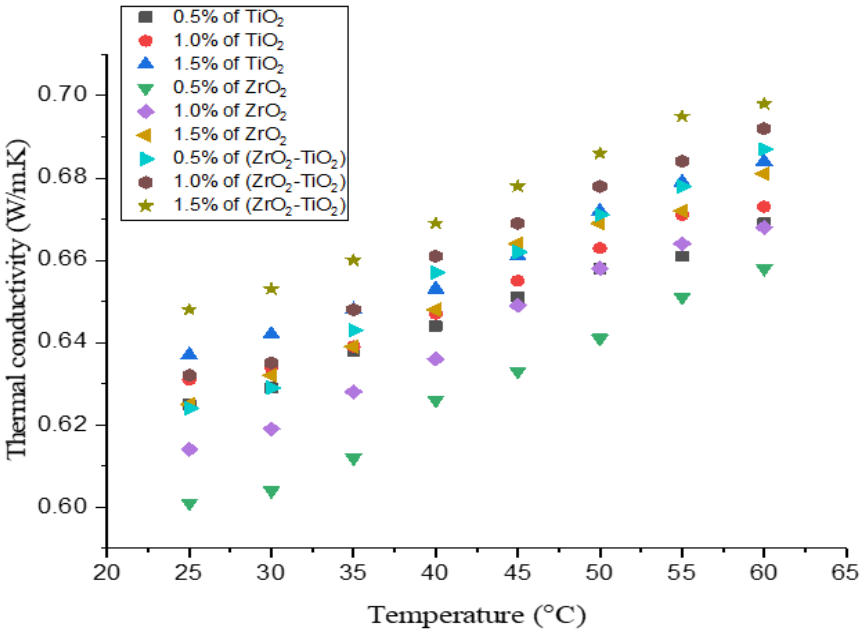

Figure 12. Changes in TC with temperature.

The TC of numerous nanofluids at varying concentrations were computed, as illustrated in **Figure 12**. TC values increased dramatically as nanoparticle concentrations increased. At lower amounts, our results correspond pretty well with the standard models. However, as concentrations rose, the TC values increased considerably with temperature, from 25 to 60 ºC.

The Thermal Conductivity (TC) enhancement shown in Equation 4 was used to compute the improved TC values of the nanofluids [19].

$$\text{TC enhancement (\%)} = \left[\frac{K_{nanofluid} - K_{basefluid}}{K_{basefluid}}\right] \times 100 \qquad \text{(Equation 4)}$$

where K = Thermal conductivity

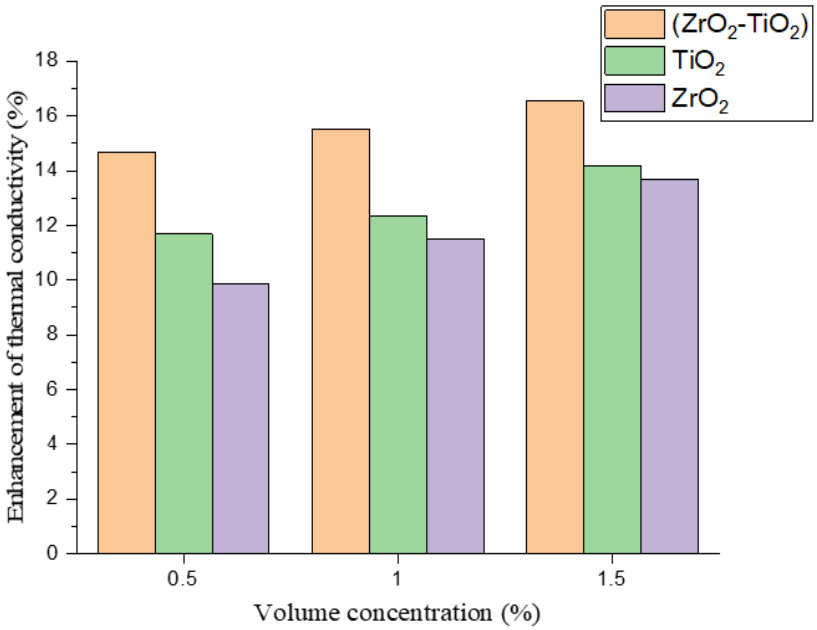

Figure 13. TC enhancement in nanofluids at various volume concentrations.

Figure 13 depicts the increase in TC of the hybrid nanofluids at various volume concentrations. Compared to ZrO_2 and TiO_2 nanofluids, the hybrid nanofluid (ZrO_2-TiO_2) performed better, with increases in TC of 14.69 %, 15.52 %, and 16.53 % at 0.5 vol%, 1.0 vol%, and 1.5 vol% concentrations of nanofluids, respectively.

Viscosity (VC) Analysis of Hybrid Nanofluids

The TC of nanofluids has been shown to increase in several earlier investigations. VC is a crucial factor to take into account when using nanofluids in practical heat management applications. The VC of nanofluids considerably influences pumping effectiveness, convection pressure drop, and heat transfer within the laminar flow. For volume fractions under 4 %, Brinkman's constructed model proved more practical and acceptable. Equation 5 demonstrates the empirical formula for Brinkman's model [34]. **Figure 14** shows the viscosity of the nanofluids at different temperature ranges. The graph shows the relationship between particle concentration and nanofluid VC.

$$\mu_{nanofluid} = \frac{\mu_{basefluid}}{(1-\phi)^{2.5}} \qquad \text{(Equation 5)}$$

where μ = Viscosity and ϕ = Volume fraction

Validation and Comparison of Results

Numerous experimental studies have proven that improving the volume concentration of the nanoparticles improves its TC. Nevertheless, the maximum or extent to which hybrid nanofluids conform to this tendency has not been determined. The results of this investigation showed that 1.5% of hybrid nanofluids obtained higher TC values compared to earlier studies [20,21].

CONCLUSION

This study used a two-step approach to create ZrO_2-TiO_2 hybrid nanofluids. The materials produced were monoclinic ZrO_2 and TiO_2, as confirmed by XRD analyses. The SEM photos demonstrated that the particles were nanometer-sized and unusually shaped. EDX revealed the ZrO_2 and TiO_2 nanoparticles' elemental composition. FTIR spectra confirmed the ZrO_2 and TiO_2 functional groups. The TC of ZrO_2-TiO_2 hybrid nanofluids was examined at volume fractions of 0.5 %, 1.0 %, and 1.5 %. The TC vs. temperature graph demonstrated that TC rose with increasing volume concentrations of 0.5 %, 1.0 %, and 1.5 %. The TC of the hybrid nanofluid (ZrO_2-TiO_2) increased by 1.5 % to 16.53 %. The VC of the ZrO_2-TiO_2 hybrid nanofluid at various particle concentrations was measured with a Brookfield DV-E viscometer.

ACKNOWLEDGEMENTS

The authors would like to express their gratitude to Pondicherry University in Puducherry for providing the resources for preparing nanofluids and, Kalasalingam Academy of Research and Education, Krishnankoil for XRD, SEM, EDX facilities & FTIR, and Karunya Institute of Technology and Sciences, Coimbatore for VC and TC measurement facilities.

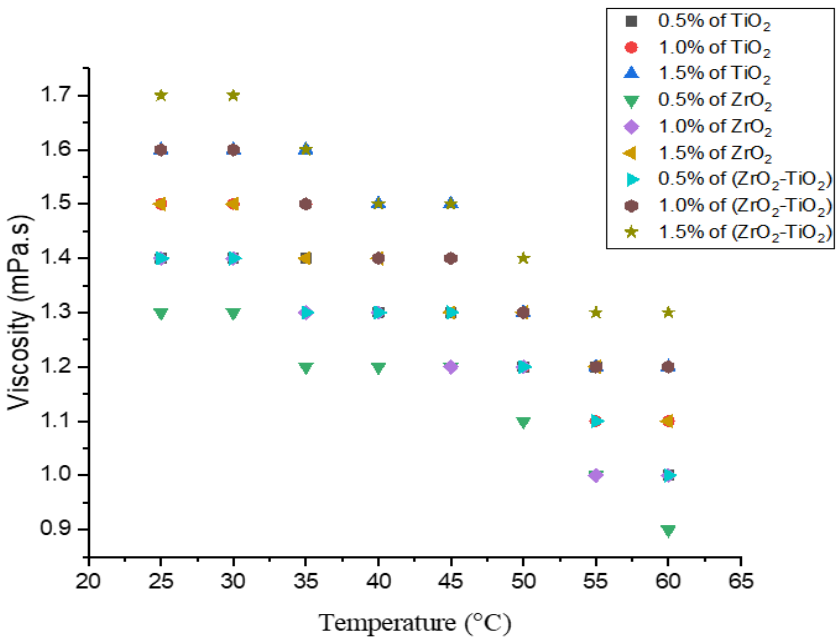

Figure 14. Variation in VC with temperature.

REFERENCES

1. Kumar, N., Sonawane, S. S. (2016) Experimental study of Fe2O3/water and Fe2O3/ethylene glycol nanofluid heat transfer enhancement in a shell and tube heat exchanger. *Int. Commun. Heat Mass Transf.*, **78**, 277–284.

2. Logesh, K., Ramesh, V., Kumar, T. P. B., Kumar, V. P., Akash, B. (2019) Preparation and property studies of SiO2/H2O nanofluid. *Mater. Today, Proc.*, **18**, 4816–4820.

3. A. J. (2015) To Conduct the Performance Test on Chiller Unit By Using Nanofluid Cooled. *Int. J. Mech. Eng. Robot. Res.*, **4**, 279–285.

4. Srinivas, T., Venu Vinod, A. (2016) Heat transfer intensification in a shell and helical coil heat exchanger using water-based nanofluids. *Chem. Eng. Process. Process Intensif.*, **102**, 1–8.

5. Kumar, P. C. M., Kumar, J., Tamilarasan, R., Sendhil Nathan, S., Suresh, S. (2014) Heat transfer enhancement and pressure drop analysis in a helically coiled tube using Al2O3 / water nanofluid. *J. Mech. Sci. Technol.*, **28**, 1841–1847.

6. Leong, K. Y., Saidur, R., Mahlia, T. M. I., Yau, Y. H. (2012) Modeling of shell and tube heat recovery exchanger operated with nanofluid based coolants. *Int. J. Heat Mass Transf.*, **55**, 808–816.

7. Suresh, S., Venkitaraj, K. P., Selvakumar, P., Chandrasekar, M. (2011) Synthesis of Al2O3-Cu/water hybrid nanofluids using two step method and its thermo physical properties. *Colloids Surfaces A Physicochem. Eng. Asp.*, **388**, 41–48.

8. Teng, T. P., Hung, Y. H. (2014) Estimation and experimental study of the density and specific heat for alumina nanofluid. *J. Exp. Nanosci.*, **9**, 707–718.

9. Hung, Y. H., Teng, T. P., Teng, T. C., Chen, J. H. (2012) Assessment of heat dissipation performance for nanofluid. *Appl. Therm. Eng.*, **32**, 132–140.

10. Fares, M., AL-Mayyahi, M., AL-Saad, M. (2020) Heat transfer analysis of a shell and tube heat exchanger operated with graphene nanofluids. *Case Stud. Therm. Eng.*, **18**, 100584.

11. Balaji, V., Arulprakasajothi, M., Logesh, K., Tharunpillai B. (2018) Assessment of heat transfer behavior of water based alumina nanofluid. *Mater. Today Proc.*, **5**, 20641–20646.

12. Jamal-Abadi, M. T., Zamzamian, A. H. (2013) Thermal conductivity of Cu and Al-water nano-fluids. *Int. J. Eng. Trans. B Appl.*, **26**, 821–828.

13. Kumar, P. M., Kumar, J., Tamilarasan, R., Sendhilnathan S., Suresh S. (2015) Review on nanofluids theoretical thermal conductivity models. *Eng. J.*, **19**, 67–83.

14. Rocha, M. S., Cabral, E. L. L., Sabundjian, G., Yoriyaz, H., Lima, C. S., Junior, A. B., et al. (2015) Characterization of Physical Properties of Al2O3 and ZrO2 Nanofluids for Heat Transfer Applications. *Int. Nucl. Atl. Conf.*, October.

15. Palanisamy, R., Parthipan, G., Palani, S. (2021) Study of synthesis, characterization and thermo physical properties of Al2O3-SiO2-TiO2 / H2O based tri-hybrid nanofluid. *Dig. J. Nanomater. Biostructures.*, **16**, 939–949.

16. Kolappan, S., Karthik, S., Logesh, K., Vasudevan, A. (2020) Thermal characterisation study of ZrO2/water nanofluid. *Int. J. Ambient Energy*, **41**, 918–921.

17. Nair, V., Parekh, A. D., Tailor, P. R. (2018) Water-based Al2O3, CuO and TiO2 nanofluids as secondary fluids for refrigeration systems: a thermal conductivity study. *J. Brazilian Soc. Mech. Sci. Eng.*, **40**.

18. Manimaran, R., Palaniradja, K., Alagumurthi, N., Sendhilnathan, S., Hussain, J. (2014) Preparation and characterization of copper oxide nanofluid for heat transfer applications. *Appl. Nanosci.*, **4**, 163–167.

19. Barai, R. M., Kumar, D., Wankhade, A. V., Sayed, A. R., Junankar, A. A. (2022) Experimental study of thermal characteristics of ZrO2/EG nanofluid for application of heat transfer. *Environ. Sci. Pollut. Res.*, 0–15.

20. Le Ba, T., Várady, Z. I., Lukács, I. E., Molnár, J., Balczár, I. A., Wongwises, S., et al. (2021) Experimental investigation of rheological properties and thermal conductivity of SiO2–P25 TiO2 hybrid nanofluids. *J. Therm. Anal. Calorim.*, **146**, 493–507.

21. Nabil, M. F., Azmi, W. H., Abdul Hamid, K., Mamat, R., Hagos, F. Y. (2017) An experimental study on the thermal conductivity and dynamic viscosity of TiO2-SiO2 nanofluids in water: Ethylene glycol mixture. *Int. Commun. Heat Mass Transf.*, **86**, 181–189.

22. Nair, V., Parekh, A. D., Tailor, P. R. (2019) Experimental investigation of thermophysical properties of R718 based nanofluids at low temperatures. *Heat Mass Transf. Und Stoffuebertragung*, **55**, 2769–2784.

23. Yarmand, H., Gharehkhani, S., Shirazi, S. F. S.,

Goodarzi, M., Amiri, A., Sarsam, W. S., et al. (2016) Study of synthesis, stability and thermo-physical properties of graphene nanoplatelet/ platinum hybrid nanofluid. *Int. Commun. Heat Mass Transf.* **77**, 15–21.

24. Das, P. K., Mallik, A. K., Ganguly, R., Santra, A. K. (2016) Synthesis and characterization of TiO2-water nanofluids with different surfactants. *Int. Commun. Heat Mass Transf.*, **75**, 341–348.

25. Chandrasekar, M., Suresh, S., Srinivasan, R., Bose, A. C. (2009) New analytical models of investigate thermal conductivity of nanofluids. *J. Nanosci. Nanotechnol*, **9**, 533–538.

26. Agarwal, R., Verma, K., Agrawal, N. K., Duchaniya, R. K., Singh, R. (2016) Synthesis, characterization, thermal conductivity and sensitivity of CuO nanofluids. *Appl. Therm. Eng.* **102**, 1024–1036.

27. Pastoriza-Gallego M. J., Lugo L., Legido J. L., Piñeiro M. M. (2011) Thermal conductivity and viscosity measurements of ethylene glycol-based al2o3 nanofluids. *Nanoscale Res. Lett.*, **6**, 1–11.

28. Ali, H. M., Babar, H., Shah, T. R., Sajid, M. U., Qasim, M. A., Javed, S. (2018) Preparation techniques of TiO2 nanofluids and challenges: A review. *Appl. Sci.*, **8**.

29. Kumar, N., Sonawane, S. S. (2016) Experimental study of thermal conductivity and convective heat transfer enhancement using CuO and TiO2 nano-particles. *Int. Commun. Heat Mass Transf.* **76**, 98–107.

30. Birlik, I., Azem, N. F. A., Yiğit, R., Erol, M., Yildirim, S., Sancakoğlu, O., et al. (2014) Preparation and Characterization of TiO 2 Nanofluid by Sol-gel Method for Cutting Tools. *J. Sci. Eng.*, **14**, 453–460.

31. Horti, N. C., Kamatagi, M. D., Nataraj, S. K., Wari, M. N., Inamdar, S. R. (2020) Structural and optical properties of zirconium oxide (ZrO2) nano-particles: Effect of calcination temperature. *Nano Express*, **1**.

32. León, A., Reuquen, P., Garín, C., Segura, R., Vargas, P., Zapata, P., et al. (2017) FTIR and raman characterization of TiO2 nanoparticles coated with polyethylene glycol as carrier for 2-methoxyes-tradiol. *Appl. Sci.*, **7**, 1–9.

33. Bruggeman (2009) Berechnung verschiedener physikalisher konstanten von heterogenen substanzen. *Ann. Der Phys.*, **5**, 160–178.

34. Brinkman, H. C. (1952) The viscosity of concentrated suspensions and solutions. *J. Chem. Phys.*, **20**, 571.

35. Santhosh Kumar, J., (2019) Texila Int. J. Nurs. 59–62.

36. Anandakumar, J., Pajaniradja, K. (2017) Kichena Improving Performance of vapour compression refrigeration system by using PCM in evaporator. *J. Chem. Pharm. Sci.*, **10**, 1599–1602.

37. Anandakumar, J., Parasuraman, N. (2017) A Review of Low Temperature Refrigerator. *Ijsart.*, **3**, 82–85.

38. Parasuraman, N., Anandakumar, J. (2017) An Experimental Analysis of Di Diesel Engine Using Cashew Nut Shell Oil. *Ijsart.*

39. Anandakumar, J., Palaniradja, K. (2021) Assessment on Performance advancement utilizing nanofluid as additional fluid in a Refrigeration System. *Int. J. Emerg. Trends Eng. Res.*, **9**, 1205–1210.